THI1, a Thiamine Thiazole Synthase, Interacts with Ca^{2+}-Dependent Protein Kinase CPK33 and Modulates the S-Type Anion Channels and Stomatal Closure in Arabidopsis[1][OPEN]

Chun-Long Li[2], Mei Wang[2], Xiao-Meng Wu, Dong-Hua Chen, Hong-Jun Lv, Jian-Lin Shen, Zhu Qiao, and Wei Zhang*

Key Laboratory of Plant Cell Engineering and Germplasm Innovation, Ministry of Education, School of Life Science, Shandong University, Jinan, 250100, China

Thiamine is required for both plant growth and development. Here, the involvement of a thiamine thiazole synthase, THI1, has been demonstrated in both guard cell abscisic acid (ABA) signaling and the drought response in Arabidopsis (*Arabidopsis thaliana*). *THI1* overexpressors proved to be more sensitive to ABA than the wild type with respect to both the activation of guard cell slow type anion channels and stomatal closure; this effectively reduced the rate of water loss from the plant and thereby enhanced its level of drought tolerance. A yeast two-hybrid strategy was used to screen a cDNA library from epidermal strips of leaves for THI1 regulatory factors, and identified CPK33, a Ca^{2+}-dependent protein kinase, as interactor with THI1 in a plasma membrane-delimited manner. Loss-of-function *cpk33* mutants were hypersensitive to ABA activation of slow type anion channels and ABA-induced stomatal closure, while the *CPK33* overexpression lines showed opposite phenotypes. CPK33 kinase activity was essential for ABA-induced stomatal closure. Consistent with their contrasting regulatory role over stomatal closure, THI1 suppressed CPK33 kinase activity in vitro. Together, our data reveal a novel regulatory role of thiamine thiazole synthase to kinase activity in guard cell signaling.

Thiamine (vitamin B1) is an essential compound for all living organisms. It contains 4-amino-5-hydroxymethyl-2-methylpyrimidine phosphate (pyrimidine) and 4-methyl-5-(2-hydroxyethyl)-thiazole phosphate (thiazole) moieties, which are synthesized separately in plastids and then coupled together to form thiamine monophosphate (Goyer, 2010; Gerdes et al., 2012). The synthesis of the former requires the product of *THIAMINC* (*THIC*; Raschke et al., 2007), while the latter is synthesized, both in Arabidopsis (*Arabidopsis thaliana*) and maize (*Zea mays*), by the single enzyme THI1 (Belanger et al., 1995; Machado et al., 1996), via a pathway which uses Gly, NAD^+, and an unknown source of sulfur (Chatterjee et al., 2007). *THI1* from Arabidopsis and yeast (*Saccharomyces cerevisiae*) were shown to be involved in mitochondrial DNA damage tolerance (Machado et al., 1996, 1997). The Arabidopsis *thi1* mutant *tz-201* forms yellow rosette leaves and requires a supply of thiamine to survive (Papini-Terzi et al., 2003). THI1 is targeted to both the mitochondrion and the chloroplast (Chabregas et al., 2001, 2003). The dual targeting of HET-P synthase may enable this enzyme to function in protection against DNA damage when targeted to mitochondria and to function in thiamine biosynthesis when targeted to chloroplasts (Ajjawi et al., 2007). Recent studies showed that *THI1* transcription was up-regulated by abiotic stresses, such as sugar deprivation, high salinity, hypoxia, and oxidative stress (Ribeiro et al., 2005; Tunc-Ozdemir et al., 2009). In addition, abscisic acid (ABA) played an important role in the up-regulation of the thiamine biosynthetic genes *THI1* and *THIC* during salt stress (Rapala-Kozik et al., 2012). These studies suggest that THI1 may play additional roles in plant abiotic stress responses besides its known functions in thiamine biosynthesis and mitochondrial DNA damage tolerance.

Plants respond to drought by synthesizing ABA, which has the effect of reducing transpirational water loss through the induction of stomatal closure (Geiger et al., 2011; Lee et al., 2013). The guard cell plasma

[1] This work was supported by the National Natural Science Foundation of China (31170236 and 31271506), the key special project "Breeding and Cultivation of Novel GM Varieties" (2014ZX08009–022B), the Program for New Century Excellent Talents in University (NCET–13–0354), and the Shandong Science Fund for Distinguished Young Scholars (2014JQE27047).

[2] These authors contributed equally to the article.

* Address correspondence to weizhang@sdu.edu.cn.

The author responsible for distribution of materials integral to the findings presented in this article in accordance with the policy described in the Instructions for Authors (www.plantphysiol.org) is: Wei Zhang (weizhang@sdu.edu.cn).

W.Z. developed the project concept; W.Z., M.W., and C.-L.L. designed the experiments; C.-L.L. performed most of the experiments and data analyses; M.W. performed some experiments; X.-M.W. and D.-H.C. examined the transgenic Arabidopsis plants; H.-J.L. performed the coimmunoprecipitation assay; J.-L.S. and Z.Q. contributed to material preparation and data analyses; M.W., C.-L.L., and W.Z. wrote the article.

[OPEN] Articles can be viewed without a subscription.

www.plantphysiol.org/cgi/doi/10.1104/pp.15.01649

 © 2016 American Society of Plant Biologists. All Rights Reserved.

membrane anion channels and outward potassium channels act as important conduits for solute efflux during stomatal closure, and the ABA activation of guard cell anion channels is essential for ABA-induced stomatal closure (Schroeder and Hedrich, 1989; Schroeder and Keller, 1992; Pei et al., 1997; Li et al., 2000; Scherzer et al., 2012; Lee et al., 2013). The production of transient cytosolic calcium signals, which are decoded by various calcium-binding proteins (DeFalco et al., 2010), forms part of the response to drought. Among the latter proteins are the calcium-dependent protein kinases (CDPKs). In Arabidopsis, for example, CPK3 and CPK6 are thought to function as Ca^{2+} sensors and positive transducers of stomatal ABA signaling (Mori et al., 2006). The *cpk4cpk11* double mutant is partially compromised with respect to ABA-induced stomatal closure (Zhu et al., 2007). In the *cpk10* mutant, the inhibition by ABA and Ca^{2+} of K^+ inward channels is compromised, resulting in ineffective stomatal closure and hence an enhanced susceptibility to drought stress (Zou et al., 2010). CPK13 inhibits the expression of the guard cell channel proteins KAT2 and KAT1 (Ronzier et al., 2014), thereby restricting stomatal aperture, while CPK21 and CPK23 function during a drought stress episode to phosphorylate and activate the S-type anion channel SLAC1 in an ABA-responsive manner (Ma and Wu, 2007; Geiger et al., 2010; Franz et al., 2011). Although the CDPKs are clearly important for the regulation of stomatal movement, the molecular basis of their activity remains obscure.

Here, it is demonstrated that THI1 is involved in ABA-regulated stomatal movement, S-type anion channels, and the plant's drought response. Subsequently, CPK33 was identified as a downstream target for THI1. A genetic and cellular analysis showed that CPK33 was also involved in the ABA-mediated regulation of stomatal closure and drought stress responses. Moreover, we found that THI1 interacts with and represses CPK33 kinase activity, indicating a new regulatory function of thiamine thiazole synthase to kinase activity of CPK in response to drought stress.

RESULTS

THI1 Is Expressed in Guard Cells and at the Plasma Membrane

As also reported by Ribeiro et al. (2005), *THI1* was expressed broadly in the root, the cotyledon, the leave, the hypocotyl, the inflorescence, and the silique (Fig. 1, A–F). Here, the gene was strongly expressed in the guard cells (Fig. 1C) and was up-regulated by both ABA treatment and exposure to drought stress, although not by thiamine treatment (Fig. 1, G–I). Accordingly, subsequent work was aimed at assessing a potential role of *THI1* in stomatal movements and drought resistance.

Previously THI1 was shown to be targeted to both mitochondria and chloroplasts (Chabregas et al., 2001, 2003; Jin et al., 2003). In mesophyll protoplasts extracted from plants carrying the p*THI1*::*THI1-GFP* transgene, GFP was deposited solely in the plastids; however, when the protoplasts were exposed to different concentrations of ABA for 6 h, plasma membrane localization of THI1 was also observed (Fig. 1, J and K; Supplemental Fig. S1). To further confirm the correlation of THI1 level and its plasma membrane localization, THI1-GFP driven by the constitutive cauliflower mosaic virus 35S promoter was introduced into mesophyll protoplasts to express transiently. As a result, p*35S*::*GFP* transgene was expressed throughout the cell (Fig. 1L), while all of the GFP signal produced by p*35S*::*THI1-GFP* was restricted to both plastid and the plasma membrane (Fig. 1M; Supplemental Fig. S2). Consistently, the p*35S*::*THI1-GFP* product colocalized with both the lypophilic dye *N*-(3-triethylammoniumpropyl)-4-(6-(4-(diethylamino) phenyl) hexatrienyl) pyridinium dibromide (FM4-64) and plasma membrane marker protein H^+-ATPase-RFP (Kim et al., 2001) at the plasma membrane (Fig. 1, N and O).

ABA-Induced Stomatal Closure and Slow Anion Currents Are Enhanced in *THI1* Overexpressors

To address whether *THI1* plays a role in the guard cell signaling, we first analyzed transformants in which *THI1* was constitutively overexpressed (THI1-OE-8 and -14). A quantitative real-time PCR (qPCR)-based assessment showed that the abundance of *THI1* transcript was substantially higher in the two OE lines than in the wild type (Columbia-0 [Col-0]; Fig. 2A). As shown in Figure 2, B and C, stomatal aperture under nonstressed conditions was similar in all three lines, but in the presence of exogenous ABA, stomatal aperture was reduced in both transgenic lines, thereby improving their tolerance of drought stress. Both the measured water loss from detached leaves and the assay of whole plant drought tolerance confirmed the superiority of the OE lines over the wild type (Fig. 2, D and E). Both the two *THI1* point mutation lines (CS3573 and CS3590) and the two RNAi-based knock-down lines (THI1-R2 and -R4) formed plants of reduced stature and developed pale leaves; they required the supply of 1 mM thiamine to maintain normal growth (Supplemental Figs. S3C and S4C). Stomatal closure did not vary between these genotypes exposed to either control conditions or to 50 μM ABA (Supplemental Figs. S3, A and B, and S4B). Similarly, there was no effect on stomatal aperture of applying a range of thiamine concentrations (Supplemental Fig. S5). These data suggested that the stomata regulatory effect of *THI1* OE lines was not due to increased thiamine biosynthesis.

Slow anion efflux channels have been proposed to play an important role during stomatal closure (Geiger et al., 2009; Lee et al., 2009; Kim et al., 2010); thus, we next examined whether ABA activation of slow anion channels differed in guard cells of wild-type and OE lines. In the absence of ABA, neither the size of the slow anion current nor the kinetics of the OE guard cells were distinguishable from those of the wild type's guard cells; however, in the presence of 50 μM ABA, markedly

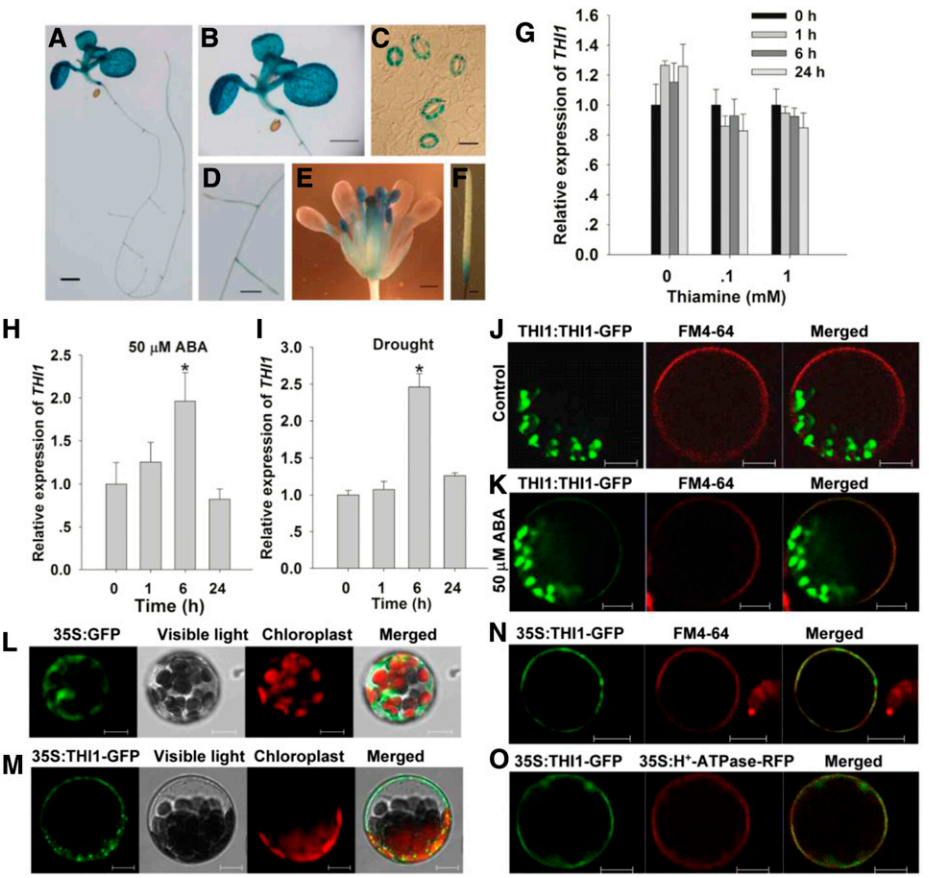

Figure 1. *THI1* expression and the subcellular localization of THI1. A to F, GUS activity produced by p*THI1*::GUS in a 10-d-old seedling (A), a leaf (B), guard cells (C), the root (D), the inflorescence (E), and the silique (F). Bars in A, B, and F = 1 mm; in C = 10 μm; and in D and E = 0.5 mm. G to I, qPCR-based assessment of *THI1* induction in the presence of thiamine (G), ABA (H), and drought stress (I). Transcript levels relative to that of the reference gene *ACTIN2* are presented, with each value being given in the form mean ± SE (n = 3). Asterisks indicate significant differences between means ($P < 0.05$). J to N, The localization of THI1 in Arabidopsis leaf protoplasts harboring p*THI1*::*THI1-GFP* in the presence of FM4-64 and control (ethanol; J), p*THI1*::*THI1-GFP* in the presence of FM4-64 and 50 μM ABA (K), p*35S*::*GFP* (L), p*35S*::*THI1-GFP* (M), and p*35S*::*THI1-GFP* in the presence of FM4-64 (N). O, The colocalization of GFP-tagged THI1 and RFP-tagged H^+-ATPase. Bars in J to O = 10 μm.

larger slow anion currents were observed in the former (Fig. 2, F and G). The conclusion was that THI1 acts as a positive regulator for the ABA-induced activation of slow type anion channels during stomatal closure.

THI1 Physically Interacts with CPK33

To identify the candidate proteins that interact with THI1, yeast two-hybrid system was applied to screen an Arabidopsis cDNA library from epidermal strips of leaves. The transformed cells were plated on synthetic dropout selection medium that lacked Trp, Leu, and His supplemented with 30 mM 3-amino-1,2,4-triazole to inhibit the self-activation of reporter genes (Supplemental Fig. S6). Among several positive clones identified, one cDNA clone, encoding Ca^{2+}-dependent protein kinase CPK33 (*At1g50700*), showed strong interaction with THI1 (Fig. 3A). *CPK33* encodes a protein of 521 amino acid residues with a kinase domain (KD) and four calcium-binding motifs (EF hands; Fig. 3B). The KD of CPK33 also interacts with THI1 in yeast cells (Fig. 3A). To explore whether THI1 enzyme activity affects the interaction between CPK33 and THI1, protein-protein interaction was detected in the presence of different concentrations of thiamine. As a result, the intensity of the interaction was unresponsive to the level of thiamine present in the medium (Supplemental Fig. S7).

To test whether THI1 interacts with CPK33 in vitro, we carried out a GST pull-down assay. Recombinant GST or CPK33-GST fusion protein, bound to glutathione-Sepharose beads, was allowed to interact with the purified THI1-His protein. CPK33-GST bound to the THI1-His fusion, whereas GST itself did not, indicating that CPK33 interacts with THI1 in vitro (Fig. 3C). To further validate the interaction between CPK33 and THI1 in planta, we transiently cotransformed *Nicotiana benthamiana* leaf cells with genes encoding Myc-tagged CPK33 and either GFP or GFP-tagged THI1. Immunoprecipitation based on an anti-GFP antibody demonstrated that CPK33-Myc was precipitated only when in the presence of both the *THI-GFP* and *CPK33-Myc* products, while in contrast, no CPK33-Myc could be detected in cells cotransformed with either *GFP* and *CPK33-Myc* or with *THI1-GFP* and *Myc* (Fig. 3D; Supplemental Fig. S8). This result confirmed that the two proteins interacted with one another in planta.

Transcription of *CPK33* and Subcellular Localization of CPK33

Since CPK33 interacted with THI1, the expectation was that the expression profiles of their encoding genes would overlap and that the two proteins would be deposited in the same subcellular space. In transgenic plants harboring p*CPK33*::*GUS*, GUS activity was

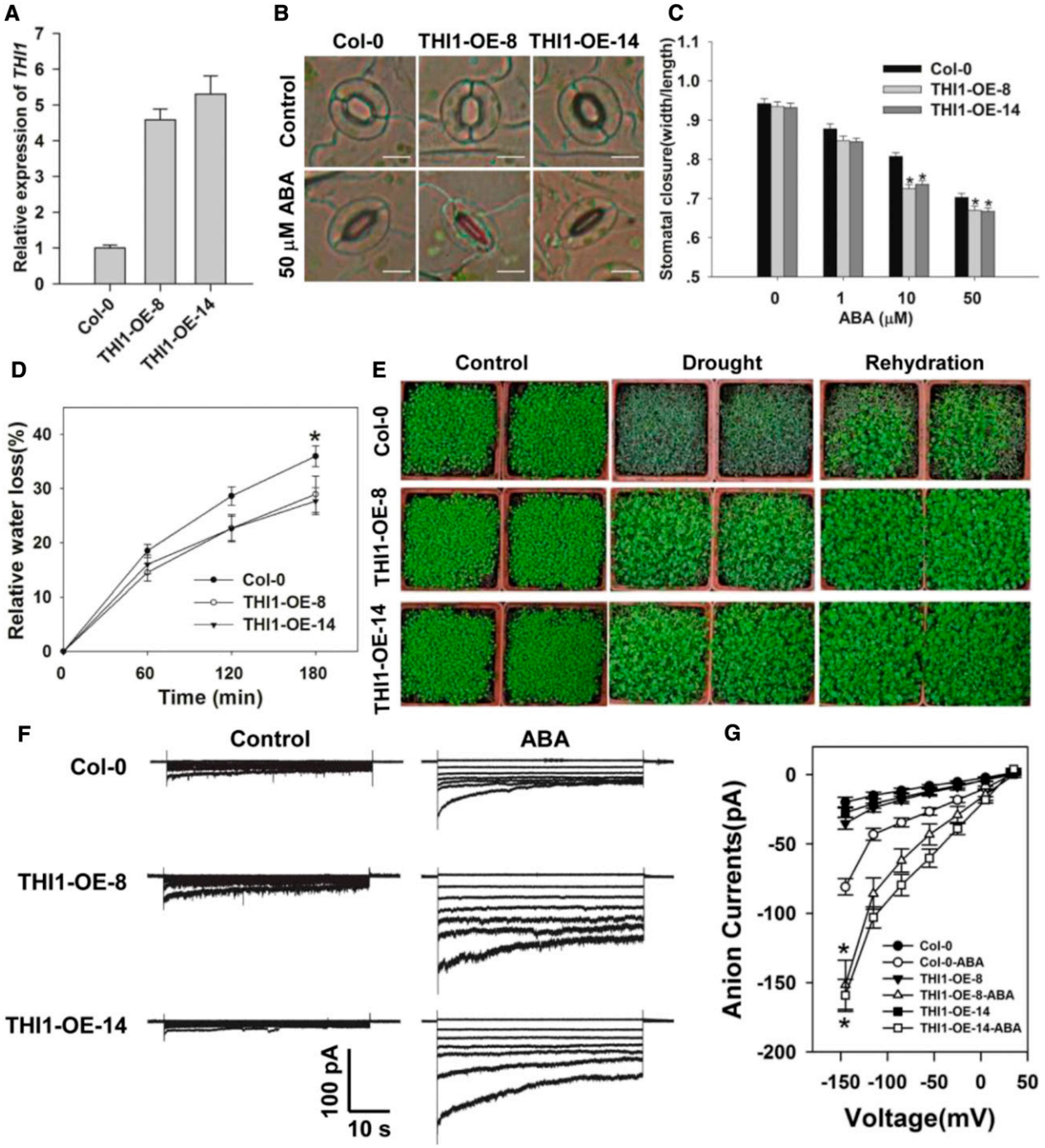

Figure 2. *THI1* overexpression increases the impact of ABA on stomatal closure and slow anion channel currents, and enhances drought tolerance. A, qPCR-based assessment of *THI1* transcription in Col-0, and the overexpression lines 8 and 14 (THI1-OE-8 and THI1-OE-14). *ACTIN2* was used as an internal control. B and C, ABA promotes stomatal closure more strongly in the overexpression lines than in the wild type. Shown: Photos (B) and width/length ratio analysis of the stomatal aperture (C). Error bars represent the SE ($n = 3$). At least 60 stomata were measured for each genotype per replication. Bar in B = 10 μm. D, The rate of water loss from detached leaves. Data presented in the form mean ± SE ($n = 3$). E, The drought response of the *THI1* overexpression lines. F, The effect of supplying 50 μM ABA on slow anion currents in the guard cell protoplasts. G, Current/voltage relationships of whole cell slow anion currents as illustrated in F. The numbers of guard cells measured were: Col-0 (13), Col-0-ABA (11), THI1-OE-8 (9), THI1-OE-8-ABA (10), THI1-OE-14 (12), and THI1-OE-14-ABA (9). Data are shown in the form mean ± SE. Asterisks in C, D, and G indicate significant differences between means ($P < 0.05$).

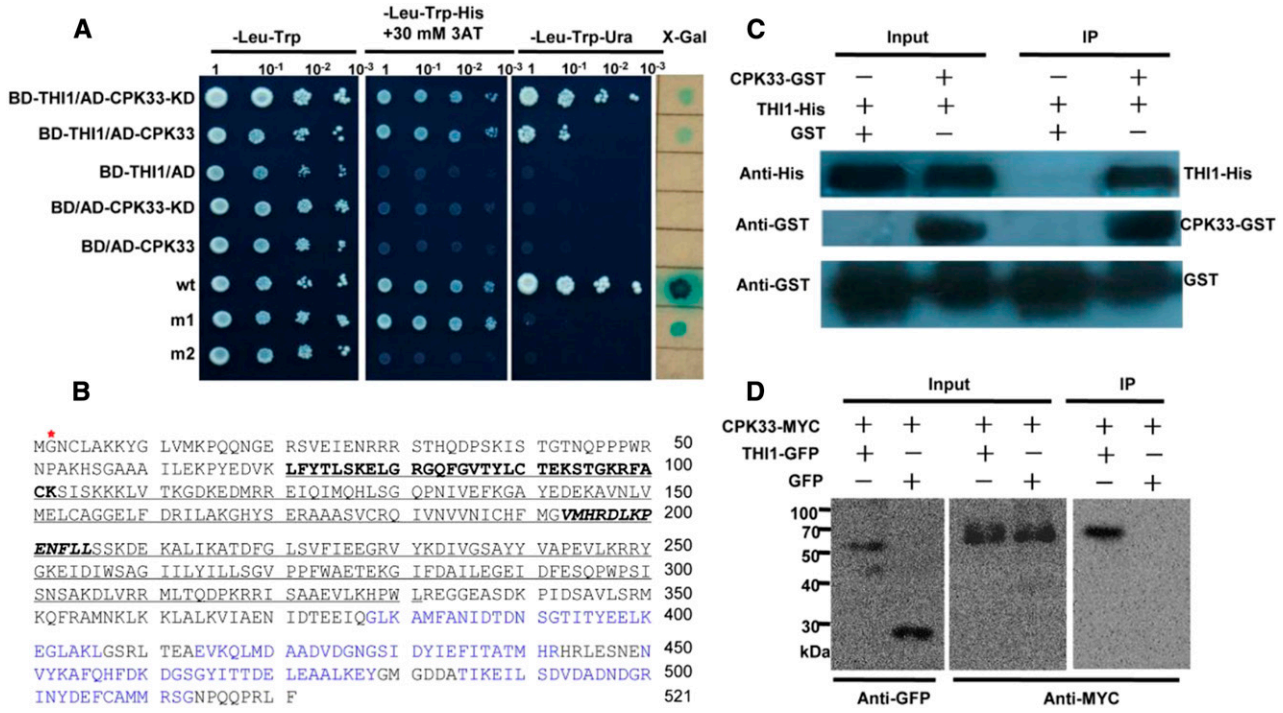

Figure 3. CPK33 interacts with THI1. A, Yeast two-hybrid assay. BD, pDEST32 is the bait plasmid; AD, pDEST22 the prey plasmid. wt (pEXP22-RalGDS-wt), m1 (pEXP22-RalGDS-m1), or m2 (pEXP22-RalGDS-m2) is control plasmid showing, respectively, a strong, weak, or nondetectable interaction with pEXP32-Krev1. KD, CPK33 KD. B, Deduced amino acid sequence of CPK33. The KD is shown underlined, the ATP-binding site in bold type, the active site in bold italic type, and the myristoylation site by a red star; The EF hands are shown in blue. C, A pull-down assay (bait protein, CPK33-GST; prey protein, His-tagged THI1) confirms the interaction between THI1 and CPK33. GST was used as the bait representing a negative control. D, In vivo coimmunoprecipitation confirms the interaction between THI1 and CPK33 in *N. benthamiana* leaves. IP, Immunoprecipitation.

present in the primary root, the leaf, the inflorescence, and the silique, and particularly strongly in the guard cells (Fig. 4, A–F), matching the pattern of *THI1* expression (Fig. 1C). Both ABA treatment and drought stress (but not thiamine supplementation) could induce the expression of *CPK33* (Fig. 4, G–I), suggesting a potential role of *CPK33* in the regulation of stomatal movements and drought stress response. In Arabidopsis mesophyll protoplasts transiently expressing a fusion of *GFP* to the *CPK33* C terminus, signal was detected at the plasma membrane (Fig. 4J). A similar localization was observed in stable transformants harboring p*CPK33*::*CPK33-GFP* (Fig. 4L). Mutation of the N-terminal Gly residue (G) at position 2 of the myristoylation site, which promoted protein-membrane interaction (Johnson et al., 1994; Cheng et al., 2002), compromised this association (Supplemental Fig. S9). It has recently been shown that CPK33 is present in the nucleus of shoot apical cells (Kawamoto et al., 2015); the inconsistence with the plasma membrane localization of CPK33 in the leaves and roots in our study may be due to the different tissues detected. When the *CPK33-GFP* transgene was cotransformed into Arabidopsis mesophyll protoplasts together with the *THI1-RFP*, the GFP and RFP signals both appeared at the plasma membrane (Fig. 4K). Thus, the CPK33-THI1 interaction likely occurs at the plasma membrane. When wild-type and *cpk33* mesophyll protoplasts were transformed with p*35S*::*THI-GFP*, it was established that the loss of function of *CPK33* had no effect on the plasma membrane localization of THI1 (Supplemental Fig. S10).

CPK33 Is a Negative Regulator of Stomatal Closure and Slow Anion Currents

Based on the findings that CPK33 is a binding partner of THI1, we next aimed to investigate whether CPK33 plays a role in the regulation of stomatal closure. To characterize the physiological role of *CPK33* in guard cells, two T-DNA insertion mutants, *cpk33-1* (SALK_036145) and *cpk33-2* (SAIL_26_C12, CS870285), were obtained from the Arabidopsis Biological Resource Center (ABRC; http://www.arabidopsis.org/abrc/). As confirmed by PCR, the T-DNA insertion in *cpk33-1* and *cpk33-2* was located in the seventh intron and sixth exon of the *CPK33* genomic DNA, respectively. Homozygous mutants were generated for further experiments (Supplemental Fig. S11, A and B). Reverse transcription (RT)-PCR experiment showed that homozygous *cpk33-1* and *cpk33-2* plants produced no full-length *CPK33* transcript (Fig. 5A; Supplemental Fig. S11C). Upon exposure to ABA, stomatal aperture in both *cpk33* mutants was notably smaller than in the wild type, but in the absence of ABA, the

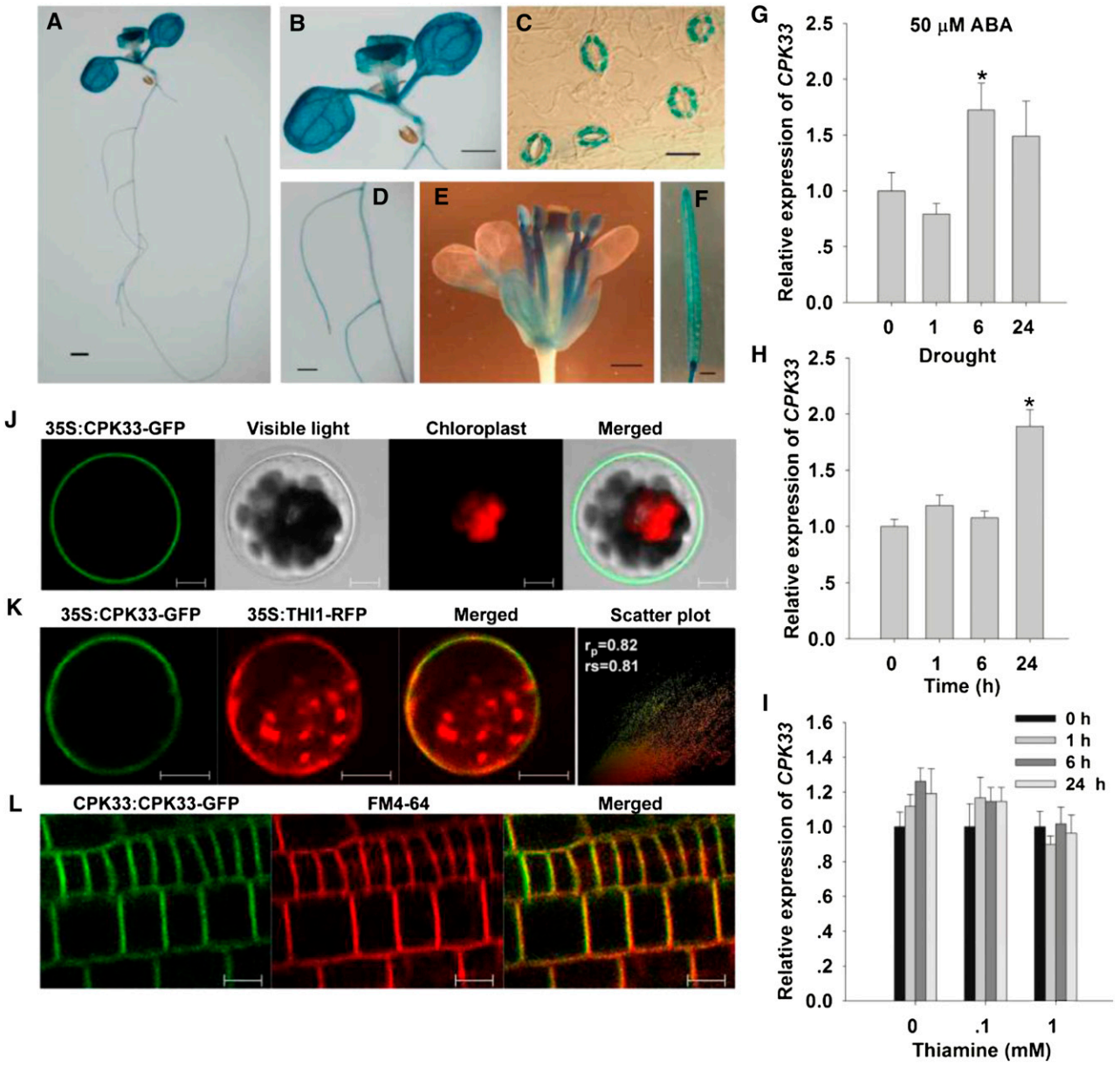

Figure 4. The expression of *CPK33* and the subcellular localization of CPK33. A to F, The behavior of plants harboring p*CPK33*::*GUS*. A, Ten-day-old seedling. B, Leaf. C, Guard cells. D, Root. E, Inflorescence. F, Silique. Bar in A, B, and F = 1 mm; in C = 10 μm; and in D and E = 0.5 mm. G to I, qPCR-based assessment of *CPK33* induction in the presence of ABA (G), drought stress (H), and thiamine (I). Transcript levels relative to that of the reference gene *ACTIN2* are presented, with each value being given in the form mean $\pm$ SE (n = 3). Asterisks indicate significant differences between means ($P < 0.05$). J, The subcellular localization of p*35S*::*CPK33-GFP* expression in leaf protoplasts. K, Colocalization of GFP-tagged CPK33 and RFP-tagged THI1. To quantify the degree of overlap between two proteins, PSC colocalization analysis was performed. The values of fluorescence pixels across the two channels are depicted in an intensity scatter plot. r_p, Linear Pearson correlation coefficient; r_s, nonlinear Spearman's rank correlation coefficient. L, The subcellular localization of p*CPK33*::*CPK33-GFP* expression in the root. Bars in J to L = 10 μm.

mutants' behavior was indistinguishable from that of the wild type (Fig. 5, B and C). Consistent with this outcome, the rate of water loss from detached leaves was lower in the mutants, and the plants were more drought tolerant than the wild type (Fig. 5, D and E). Exposure to 50 μM ABA increased the magnitude of the slow anion currents more substantially in the mutants' than in the wild type's guard cells (Fig. 5, F and G). This result indicated that the ABA-activated slow anion currents were negatively regulated by CPK33.

To further confirm that the increased sensitivity of the *cpk33* mutants to ABA-induced stomatal closure resulted from the disruption of *CPK33* transcription, *CPK33* overexpressing lines (CPK33-OE-1 and -2) were

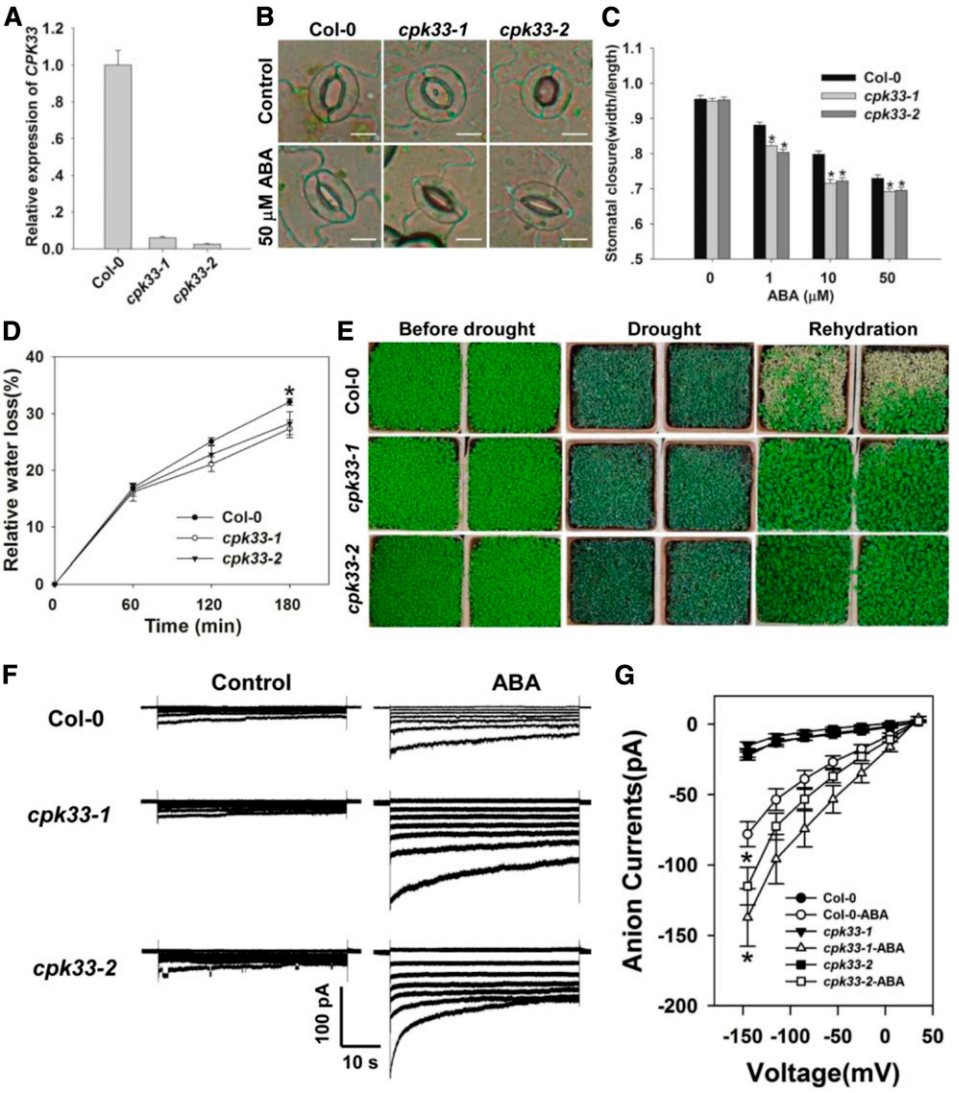

Figure 5. *CPK33* knockouts are more sensitive to ABA with respect to stomatal closure and the slow type anion channel activity, and are more drought tolerant. A, qPCR-based assessment of *CPK33* transcription in Col-0 and *cpk33* mutants. *ACTIN2* was used as an internal control. B and C, ABA promotes stomatal closure more strongly in the *cpk33* mutants than in Col-0. Shown: Photos (B) and width/length ratio analysis of the stomatal aperture (C). Error bars represent the SE ($n = 3$). At least 60 stomata were measured for each genotype per replication. Bar in B = 10 μm. D, The rate of water loss from detached leaves of the Col-0 and *cpk33* mutants. Data are in the form mean ± SE ($n = 3$). E, The *cpk33* mutants exhibited an enhanced level of drought tolerance. The experiments were repeated three times with similar results. F, ABA (50 μM) activation of slow type anion channels in Col-0 and *cpk33* mutant guard cell protoplasts. Time and voltage scales are as shown. G, Current/voltage relationships of whole-cell slow anion currents as illustrated in F. The numbers of guard cells measured were: Col-0 (13), Col-0-ABA (10), *cpk33-1* (9), *cpk33-1*-ABA (10), *cpk33-2* (12), and *cpk33-2*-ABA (9). Data are shown in the form mean ± SE. Asterisks in C, D, and G indicate significant differences between means ($P < 0.05$).

generated. qPCR experiments showed that the abundance of *CPK33* transcript was substantially higher in the two OE lines than in the wild type (Fig. 6A). Consistent with our expectations, the OE lines showed an ABA-hyposensitive phenotype in ABA promotion of stomatal closure (Fig. 6, B and C), the rate of water loss from detached leaves, drought tolerance (Fig. 6, D and E), and ABA activation of slow anion currents (Fig. 6, F and G), in line with the notion that CPK33 acts to suppress ABA-regulated stomatal closure and slow anion channel activity.

CPK33 Encodes a Ca^{2+}-Dependent Protein Kinase, and the Kinase Activity Is Essential for Its Biological Function

To confirm the kinase activity of CPK33, we expressed and purified a GST binding protein (GST)-CPK33 recombinant protein from *Escherichia coli* (BL21) cells. The purified protein exhibited autophosphorylation activity in the presence of 1 mM Ca^{2+}; it was also able to phosphorylate MBP substrate (Fig. 7A). However, no kinase activity could be detected in $CPK33^{K102R}$-GST (Fig. 7B; Supplemental Fig. S12), in which a conserved Lys residue (K) at the position 102 of the ATP binding site in the KD II was replaced with an Arg residue (R; Supplemental Figs. S13 and S14). These data indicate that CPK33 is indeed a Ca^{2+}-dependent protein kinase and its ATP binding site is indispensable for kinase activity. To investigate whether the kinase activity of CPK33 is required for its in vivo function, we produced transformants in which *cpk33-1* was complemented with a functional copy of *CPK33* or a mutated one ($CPK33^{K102R}$). The former exhibited the wild-type phenotype, whereas the latter shared the ABA-hypersensitive phenotype shown by the *cpk33* mutants (Fig. 7, C–E). Thus, CPK33's kinase activity appears to be essential for its regulation of slow anion channel activity and stomatal movement.

THI1 Represses the Kinase Activity of CPK33

When recombinant THI1-His was used as a kinase substrate for CPK33 in vitro, there was no evidence of its phosphorylation (Fig. 8A). Given that *THI1*

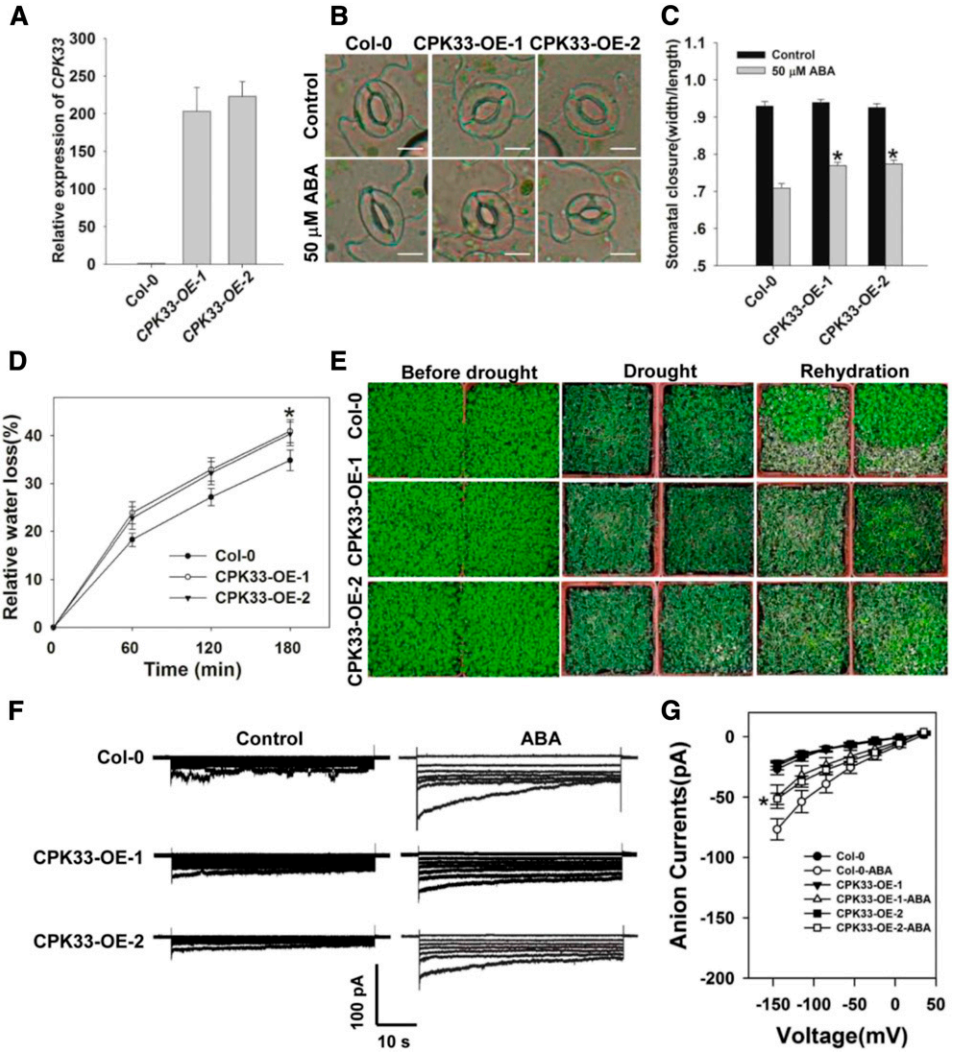

Figure 6. *CPK33* overexpression resulted in ABA hyposensitivity of guard cell movement, slow anion channel regulation, and decreased drought tolerance. A, qPCR-based assessment of *CPK33* expression in Col-0 and overexpression lines 1 and 2 (CPK33-OE-1 and CPK33-OE-2). *ACTIN2* was used as an internal control. B and C, ABA-induced promotion of stomatal closure in Col-0 and *CPK33* overexpression lines. Shown: Photos (B) and width/length ratio analysis of the stomatal aperture (C). Error bars represent the SE ($n = 3$). At least 60 stomata were measured for each genotype per replication. Bar in B = 10 μm. D, Water loss rates from detached leaves of Col-0 and *CPK33* overexpression lines. Error bars represent the SE ($n = 3$). E, Decreased tolerance to drought in *CPK33* overexpression lines. The experiments were repeated three times with similar results. F, Patch-clamp whole-cell recordings of the slow anion currents in guard cell protoplasts isolated from Col-0 and *CPK33* overexpression lines with or without 50 μM ABA. Time and voltage scales are as shown. G, Current/voltage relationships of whole-cell slow anion currents as illustrated in F. The numbers of guard cells measured were: Col-0 (8), Col-0-ABA (8), CPK33-OE-1 (7), CPK33-OE-1-ABA (7), CPK33-OE-2 (9), and CPK33-OE-2-ABA (10). Data are shown in the form mean ± SE. Asterisks in C, D, and G indicate significant differences between means ($P < 0.05$).

overexpressing transgenic lines exhibited the same ABA hypersensitivity phenotypes in stomatal closure and slow anion channels as did the *cpk33* mutants, the possibility was considered that THI1 is able to negatively regulate the kinase activity of CPK33. To test this hypothesis, increasing concentrations of THI1-His protein (0.1, 1, 10, and 50 μg) were added to the kinase buffer containing a given concentration of CPK33-GST. As shown in Figure 8, B and C, the autophosphorylation activity of CPK33-GST was repressed by THI1-His. In contrast, transphosphorylation of MBP substrate remained unaffected (Fig. 8, D and E). The conclusion was that THI1 is able to negatively regulate the autophosphorylation activity of CPK33.

DISCUSSION

THI1 is involved in synthesis of the thiamine precursor thiazole and has a role in protecting against damage to mitochondrial DNA (Machado et al., 1996,

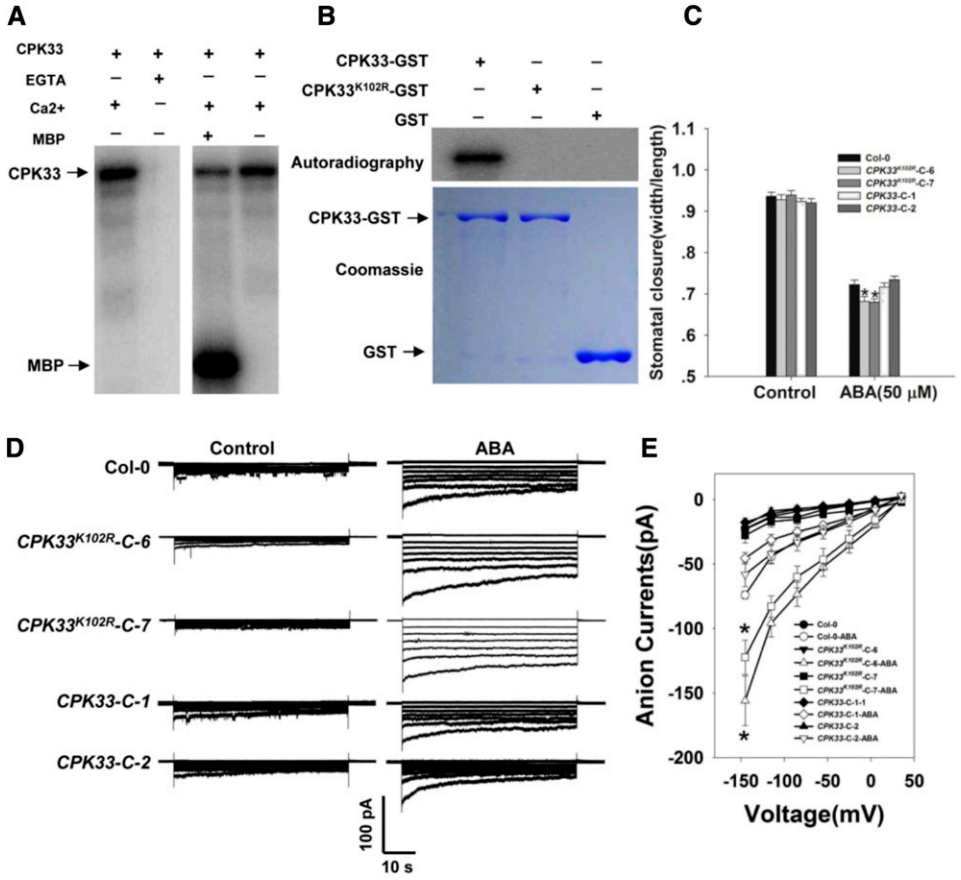

Figure 7. The kinase activity of CPK33 is required for stomatal closure and the regulation of slow type anion channels. A, In vitro assay of CPK33 kinase activity. Left: Lanes 1 and 2 show the autophosphorylation activity of CPK33-GST in the presence/absence of 1 mM free Ca^{2+} and the presence of 2 mM EGTA. Right: Lanes 3 and 4 show the phosphorylation of MBP by CPK33-GST. B, In vitro kinase activity of $CPK33^{K102R}$. Top: The autophosphorylation of purified CPK33-GST and $CPK33^{K102R}$-GST. Bottom: SDS-PAGE separation of purified CPK33-GST, $CPK33^{K102R}$-GST, and GST (arrowed). C, ABA-promoted stomatal closure. Error bars represent the SE ($n = 3$). At least 60 stomata were measured for each genotype per replication. D, ABA-activated slow type anion channels in guard cell protoplasts. Time and voltage scales are as shown. E, Current/voltage relationships of whole-cell slow anion currents as illustrated in D. The numbers of guard cells measured were: Col-0 (10), Col-0-ABA (9), CPK33-C-1 (8), CPK33-C-1-ABA (8), CPK33-C-2 (8), CPK33-C-2-ABA (9), $CPK33^{K102R}$-C-6 (9), $CPK33^{K102R}$-C-6-ABA (8), $CPK33^{K102R}$-C-7 (7), and $CPK33^{K102R}$-C-7-ABA (10). Data are shown in the form mean ± SE. Asterisks in C and E indicate significant differences between means ($P < 0.05$).

1997; Papini-Terzi et al., 2003). In Arabidopsis, *THI1* is up-regulated by various abiotic stress agents (Ribeiro et al., 2005; Rapala-Kozik et al., 2012). Here, it has been demonstrated that THI1 also has a regulatory role over stomatal closure during an episode of drought stress. Direct evidence has also been provided to show that THI1 interacts with Ca^{2+}-dependent CPK33 and represses its kinase activity, thereby functioning in guard cell signaling.

THI1 Acts as a Positive Regulator of Stomatal Closure

THI1 transcript is largely confined to green tissue (Belanger et al., 1995; Papini-Terzi et al., 2003; Ribeiro et al., 2005). The present experiments have demonstrated that this also includes the guard cells (Fig. 1C), suggesting a role of *THI1* in guard cell movements and drought stress, which was born out experimentally (Fig. 2, B–E). ABA activation of slow type anion channels mediates anionic solute efflux, as well as membrane depolarization to drive K^+ efflux, as consequently to close stomata (Hedrich et al., 1990; Grabov et al., 1997; Macrobbie, 1997; Pei et al., 1997; Li et al., 2000; Pandey et al., 2007; Acharya et al., 2013). Consistent with the ABA-induced stomatal closure results, the slow anion currents in the guard cells of *THI1* OE lines were ABA hypersensitive (Fig. 2, F and G). This provides evidence that overexpression of *THI1* enhances the plant's sensitivity to ABA and improve its tolerance to drought stress.

THI1 is targeted to both the mitochondrion and the chloroplast (Chabregas et al., 2001, 2003; Jin et al., 2003). Consistent with the previous results, only punctate distribution was found when pTHI1::*THI-GFP* was stably expressed in Arabidopsis. When plants were exposed to 50 μM ABA, *THI1* was up-regulated and its product was deposited at the plasma membrane

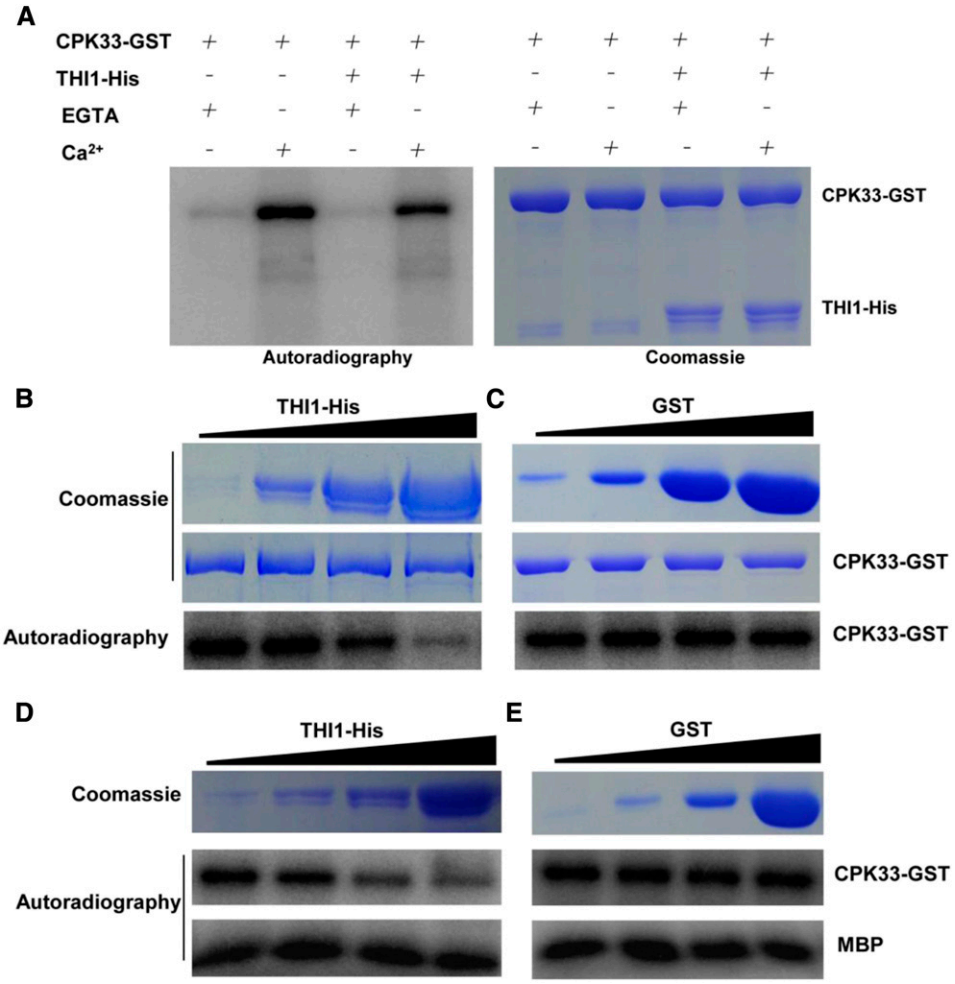

Figure 8. THI1 represses CPK33 kinase activity in vitro. A, Phosphorylation of THI1-His by CPK33-GST was detected in the presence/absence of 1 mM free Ca^{2+} and the presence of 2 mM EGTA. Left: The autophosphorylation activity of CPK33-GST was repressed by THI1-His, whereas CPK33-GST was unable to phosphorylate THI1-His. Right: SDS-PAGE separation of purified THI1-His and CPK33-GST. B and C, CPK33-GST activity in the presence of increasing concentrations of THI1-His protein (0.1, 1, 10, and 50 μg; indicated by the triangle) or GST control. Top: SDS-PAGE separation of purified proteins. Bottom: The in vitro autophosphorylation of CPK33-GST in the presence of THI1-His (B) and GST (C). D and E, THI1 represses CPK33 autophosphorylation activity but not the transphosphorylation of MBP. CPK33-GST was incubated with either increasing concentrations of THI1-His (D) or with GST (E). Top: SDS-PAGE separation of purified proteins. Bottom: The in vitro autophosphorylation of CPK33-GST in the presence of THI1-His (D) and GST (E).

(Fig. 1, H, J, and K). The possibility that an increased abundance of THI1 may encourage its deposition at the plasma membrane was supported by the behavior of plants constitutively expressing p35S::*THI1-GFP* (Fig. 1, M–O). Although THI1 does not harbor any transmembrane domains or signal peptides, several *N*-myristoylation sites are present (http://prosite.expasy.org/scanprosite/), which could allow for its posttranslational modification through the addition of myristate. Note that about half of the plasma membrane proteins identified in *Entamoeba histolytica* lack recognized transmembrane domains or membrane association sites (Biller et al., 2014). Whether THI1 is targeted to the plasma membrane via the addition of myristate and/or via its interaction with other plasma membrane protein(s) remains to be elucidated.

CPK33 Acts as Negative Regulator of Stomatal Closure

A number of CDPKs are involved in Ca^{2+}-mediated stomatal movement (Pei et al., 1996; Mori et al., 2006; Zhu et al., 2007; Zou et al., 2010; Ronzier et al., 2014). CPK33 has been identified here as an interactor with THI1 (Fig. 3) and to function as a negative regulator of ABA-induced stomatal closure (Figs. 5 and 6). The Ca^{2+}-dependent activation of anion channel currents is a key early step in the process of ABA-mediated stomatal closure (Scherzer et al., 2012). Consistent with this observation, the loss of function of *CPK33* resulted in an enhancement of ABA-induced slow anion currents, while its overexpression had the opposite effect (Figs. 5, F and G, and 6, F and G). An in vitro kinase assay indicated that CPK33 has autophosphorylation as well as transphosphorylation activity when supplied with the generic kinase substrate MBP (Fig. 7). The implication is therefore that CPK33 activity in the guard cells acts as a Ca^{2+} sensor, thereby sharing in the regulation of stomatal movement. CPK21 and CPK23, when phosphorylated, have been shown to activate the SLAC1 guard cell slow anion channel (Geiger et al., 2010). Meanwhile, CPK13 specifically inhibits KAT1 and KAT2 channel activity, thereby limiting stomatal aperture (Ronzier et al., 2014). Both CPK4 and CPK11 function in ABA signaling pathways via their capacity to phosphorylate the ABA-responsive transcription factors ABF1 and ABF4 (Zhu et al., 2007). CPK33 was unable to phosphorylate THI1 in vitro (Fig. 8A), suggesting that

THI1 cannot be its in vivo substrate; thus, further work is needed to identify its downstream targets.

THI1 Inhibits the Kinase Activity of CPK33

The overexpression of $CPK33^{K102R}$, which lacks kinase activity, failed to rescue the *cpk33* phenotype (Fig. 7, C–E), demonstrating that the kinase activity of CPK33 is essential for its function. The regulation of CDPK activity has not been extensively researched. It is known that specific phospholipids can enhance the capacity of various CDPKs to phosphorylate specific substrates (Schaller et al., 1992; Farmer and Choi, 1999), while 14-3-3 isoforms have been demonstrated to bind to and activate AtCPK1 in the presence of Ca^{2+} (Camoni et al., 1998). A *Drosophila* MAGUK (membrane-associated guanylate kinase) protein has been shown to inhibit the autophosphorylation of CaMKII at rather low Ca^{2+} levels, thereby rendering it Ca^{2+} insensitive (Lu et al., 2003). Here, in vitro assays based on purified proteins showed that the Ca^{2+}-dependent kinase autophosphorylation activity of CPK33 was repressed by THI1 in the presence of Ca^{2+} (Fig. 8), suggesting a possible novel role for THI1 in the regulation of CDPK activity. The observation that the *THI1* overexpression lines and *CPK33* loss-of-function mutants exhibited the same increased ABA sensitivity with respect to stomatal closure and anion channel currents further supported the suggestion that THI1 acts as a negative regulator of CPK33. Despite the fact that autophosphorylation of CPK33 was repressed by THI1, the autophosphorylation sites and the physiological significance of autophosphorylation of CPK33 await further classification. THI1 does not inhibit the CPK33-enacted phosphorylation of MBP (Fig. 8, D and E), but it can't be excluded yet that the potential phosphorylation of downstream targets by CPK33 is inhibited by THI1.

Consistent with the lack of any effect of exogenously applying thiamine either on the abundance of either *THI1* or *CPK33* transcript, or on the interaction between their products (Figs. 1G and 4I; Supplemental Fig. S7), thiamine treatment had no influence over stomatal movement (Supplemental Fig. S5). The implication is that the stomatal behavior of the *THI1* overexpression lines was not due to an increased synthesis of thiamine but rather resulted from the negative regulation of CPK33 kinase activity at the plasma membrane. The extent of stomatal aperture in the *THI1* RNAi knockdown and knockout lines was indistinguishable from that displayed by wild-type plants (Supplemental Figs. S3 and S4), suggesting that the basal level of THI1 is insufficient to inhibit CPK33 activity. Alternatively, binding of THI1 to CPK33 stabilizes the protein complex, which enables the repression of CPK33 autophosphorylation by THI1, and CPK33 autophosphorylation might be repressed by other regulators in the absence of THI1; thus, loss of function of *THI1* did not produce visible phenotype of stomatal movements. THI1 transcript levels responded to both ABA treatment and drought stress, particularly at the early stages of the stress response (Fig. 1, H and I), which suggested that other, as yet unidentified, mediators are likely involved in the regulation of CPK33 activity. However, further work is needed to identify the protein stability of CPK33. The transcript levels of both *THI1* and *CPK33* were up-regulated under drought stress (Figs. 1I and 4H). Generally, the negative regulators are down-regulated under such conditions; however, some regulators are up-regulated. A typical example is group A 2C type protein phosphatases, whose transcripts are accumulated to a greater extent in the presence of ABA, but they play a role as negative regulators of ABA (Verslues and Bray, 2006; Lee and Luan, 2012). Our data suggested that plant tries to induce the expression of both positive and negative regulators of ABA signaling to balance the gene regulation at the initial stage of drought stress, and that THI1 plays a role in the rapid recovery of growth and development via the negative regulation of CPK33 when the environmental condition is changed and is favorable for plant growth.

Overall, the evidence is that THI1 functions as a positive regulator of ABA signaling in guard cell, via its negative regulation of CPK33 during ABA-induced stomatal closure, and slow type anion channel activation under drought stress (Fig. 9). The indication is that this thiamine synthesis gene contributes to the regulation of slow anion channels at the plasma membrane via controlling the kinase activity of a specific CDPK. These properties suggest *THI1* as a potentially valuable candidate for manipulating the plant drought response.

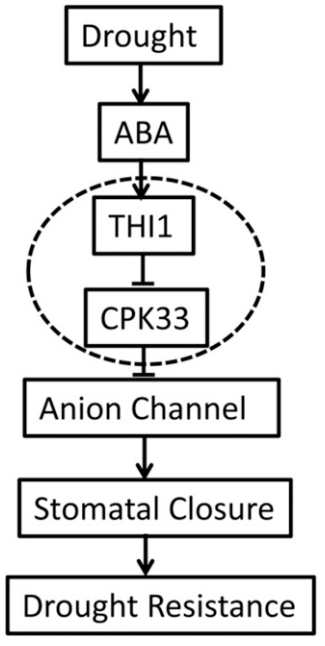

Figure 9. Hypothetical model of the process of THI1-regulated, ABA-mediated stomatal closure. Solid lines with arrows denote positive regulation, and short lines denote negative regulation.

MATERIALS AND METHODS

Plant Materials and Growth Conditions

Arabidopsis (*Arabidopsis thaliana*) ecotype Col-0 was used for this study. The Salk T-DNA insertion mutants *cpk33-1* (SALK_036145) and *cpk33-2* (CS870285) in Col-0 background (Alonso et al., 2003) were obtained from ABRC (http://abrc.osu.edu/). The T-DNA insertion position and homozygous lines of *cpk33* were identified by PCR using the primers listed in Supplemental Table S1. For seedling growth, seeds were surface-sterilized and plated on 0.7% (w/v) agar containing half-strength Murashige and Skoog (1/2 MS) medium. After low temperature vernalization at 4°C in the dark for 3 d, seeds were transferred to a growth chamber (100 μmol m^{-2} s^{-1} light, 8-h-light/16-h-dark cycle; approximate 70% relative humidity; 22 ± 1°C/16 ± 4°C day/night cycles) for further growth. About 2 weeks later, seedlings were transplanted to pots containing soil mixture (rich soil: vermiculite, 2:1, v/v).

Stomatal Closure Assay

Fully expanded young leaves from 4- to 5-week-old plants (grown under the condition as mentioned above) were harvested for stomatal aperture measurements as described previously (Acharya et al., 2013; Li et al., 2014). Leaves were floated in closure solution (20 mM KCl, 1 mM $CaCl_2$, 5 mM MES-KOH, pH 6.15) and kept in the light (room temperature; 450 μmol m^{-2} s^{-1}) for 2.5 h. Then 1, 10, or 50 μM ABA or ethanol control was added to the buffer and leaves were incubated under the same culture condition for another 2.5 h. Then the abaxial epidermal stripes were quickly peeled to make slides and photographed randomly with a light microscope (Olympus SZX16) at a total magnification of 400×. After image acquisition, stomatal widths and lengths were measured with the open access software Image J (Version 1.37), and stomatal apertures were determined as the ratio of stomatal width to length (Savvides et al., 2012).

Guard Cell Isolation and Electrophysiology

Arabidopsis guard cell protoplasts were isolated according to Zhang et al. (Zhang et al., 2008) with minor modification. Briefly, the abaxial epidermis were peeled from five to 10 fully expanded young leaves of 4-week-old Arabidopsis plants and then blended in 500 mL of distilled water for 30 s. The peels were filtered through a 100-μm nylon mesh and put into 5 mL of enzyme solution I, which contained 0.7% cellulysin cellulase, 0.1% PVP 40, 0.25% BSA in 55% basic solution (5 mM MES, 0.5 mM $CaCl_2$, 0.5 mM $MgCl_2$, 0.5 mM ascorbic acid, 10 μM KH_2PO_4, 0.55 M sorbitol, pH 5.5). The peels were digested in a shaking water bath at 120 rpm for 30 min at 28°C. After 5 mL of basic solution was added and shaken for another 5 min, the partially digested peels were collected through a 100-μm nylon mesh and put into 5 mL of enzyme solution II, which contained 1.5% Onuzuka cellulase RS, 0.02% cellulase Y-23, 0.25% BSA in 100% basic solution. After digestion by shaking at 60 rpm for at least 30 min at 22°C, the peels were mixed by pipetting up and down with a 1-mL pipette and filtered through 30-μm nylon mesh. The protoplasts were centrifuged at 800 rpm for 5 min and washed twice by basic solution.

The whole-cell mode was used for patch-clamp electrophysiology as described previously (Pei et al., 1997; Wang et al., 2001; Acharya et al., 2013). To measure slow anion channel currents, the pipette solution contained 150 mM CsCl, 2 mM $MgCl_2$, 6.7 mM EDTA, 3.35 mM $CaCl_2$, and 10 mM HEPES (pH 7.5), the bath solution contained 2 mM $MgCl_2$, 30 mM CsCl, 10 mM MES-Tris (pH 5.6), and 1 mM $CaCl_2$. Osmolarity of the solutions was adjusted with sorbitol to 500 and 480 mOsm for pipette and bath solutions. The ATP (Mg-ATP 10 mM) and GTP (10 mM) were added into the pipette solution before use from stock solutions every time. The whole-cell currents were recorded using an Axopatch-200B amplifier (Axon Instruments) 5 min after the whole-cell configuration was achieved. The holding potential was +30 mV, and voltage steps were applied from –145 to +35 mV with +30-mV increments, with a 60-s duration for each test voltage. For the ABA treatment, guard cell protoplasts were treated with 50 μM ABA for 2 h before recording, and 50 μM ABA also was added into pipette and bath solutions when recording. pCLAMP software (version 10.2; Axon Instruments) was used to acquire and analyze the whole-cell currents. SigmaPlot 11.0 software was used to draw current density voltage plots and for data analysis.

Promoter GUS Fusions and the Detection of Transgene Activity

The 1,015-bp native *THI1* promoter (part of *At5g54770*) and the native 1,131-bp *CPK33* promoter (*At1g50700*) were amplified by PCR using the primer pairs *THI1*proF/proR and *CPK33*proF/proR, respectively (Supplemental Table S1). The amplicons were inserted into the *Hin*dIII and *Bam*HI sites of the pCambia-ubiGus binary vector, replacing the *Ubiquitin* promoter, to generate the constructs p*THI1*::*GUS* and p*CPK33*::*GUS*. The constructs were introduced separately into *Agrobacterium tumefaciens* strain GV3101, then transformed into Arabidopsis using the floral dip technique (Clough and Bent, 1998). The selected T_3 homozygous transgenic seedlings were used for GUS staining assay. Transgenic plant tissues were immersed in a GUS staining solution (2 mM X-Gluc, 2 mM $K_3Fe(CN)_6$, 2 mM $K_4Fe(CN)_6$, 0.1% Triton X-100, and 10 mM EDTA in 50 mM sodium phosphate buffer, pH 7.2) and incubated at 37°C for 5 h, followed by transferring into 70% (v/v) ethanol to remove chlorophyll. The decolorized tissues were observed by Olympus SZX16 microscope and photographed by digital camera E-620 (Olympus).

Subcellular Localization and Colocalization

The transient expression of THI in Arabidopsis protoplasts was analyzed by introducing the transgene construct p*35S*::*THI1-GFP* or p*35S*::*THI1-RFP*. The *THI1* open reading frame (ORF) was amplified and cloned into either pBI221-GFP (Liu et al., 2014) or pAVA321-RFP. $CPK33^{G2A}$ was generated by site-directed mutagenesis PCR (Ho et al., 1989). The *CPK33* and $CPK33^{G2A}$ ORFs were cloned into pBI221-GFP to generate p*35S*::CPK33-GFP and p*35S*::$CPK33^{G2A}$*-GFP*. After purification using a NucleoBond Xtra Midi kit (Macherey-Nagel; www.mn-net.com), the recombined plasmids were introduced into Arabidopsis mesophyll protoplasts, following Sheen (2001), which were then held overnight in the dark at 23°C. The p*THI1*::*THI1*-GFP and p*CPK33*::*CPK33*-GFP constructs were obtained by digesting pBI221-GFP with *Bam*HI and *Eco*RI and then replacing *GUS* with the construct. The ORF sequence amplified by the primer pair *THII*-Y2HF/R was cloned into the pB7WGF2.0 binary vector to generate p*35S*::*THI1*-GFP. The GFP signal and chlorophyll autofluorescence were examined using a confocal laser-scanning microscope (LSM 700; Carl Zeiss; microscopic imaging platform of Shandong University) at excitation wavelengths of 488 and 647 nm, respectively. Red signal was obtained with an excitation at 543 nm and emission at 615 nm. The overlap of images was analyzed using Pearson and Spearman correlation coefficient colocalization plug-in of the Image J analysis program (French et al., 2008). The threshold level was set to 10, below which pixel values were considered noise and excluded in the statistical analysis. The primers used are listed in Supplemental Table S1.

RT-PCR and qPCR

To analyze the transcript levels of *THI1* and *CPK33* in response to thiamine, ABA, or drought stress, 3-week-old seedlings (Col-0) grown on 1/2 MS agar plates were transferred to 1/2 MS solution and incubated for additional 24 h. Then, 0.1 mM, 1 mM thiamine, or 50 μM ABA was added and incubated for 1, 6, or 24 h. Drought treatment was conducted by exposure of 3-week-old seedlings in growth chamber for 1, 6, or 24 h. At indicated times after initiation of each treatment, seedlings were harvested and frozen in liquid nitrogen immediately. Total RNA was isolated from Arabidopsis seedlings using TRIzol reagent (Takara), then treated with RNase-free DNase I (Promega). cDNA was subsequently synthesized from 1 μg of total RNA by using RevertAid First Strand cDNA Synthesis Kit (Thermo) and oligo(dT) as primers. RT-PCR was conducted following the supplier's protocol (Takara). qPCR experiments were performed using SYBR Premix Ex Taq mix (Takara) with gene-specific primers and internal control (*ACTIN2*). Primers used are listed in Supplemental Table S1.

Identification of T-DNA Insertion Mutants and Construction of Transgenic Plants

The T-DNA insertion position and homozygous lines of *cpk33-1* and *cpk33-2* were identified by PCR using a combination of a gene-specific primer and a T-DNA border primer (LBb1.3, LB2). To construct the plasmids *35S*::*CPK33* and *35S*::$CPK33^{K102R}$ for overexpression in Arabidopsis and *cpk33* mutant, the DNA fragment containing the entire ORF of *CPK33* or $CPK33^{K102R}$ was double digested with *Bam*HI/*Sac*I and ligated into the pSTART vector. *CPK33* was

amplified with primers *CPK33*OE-F and *CPK33*OE-R. *CPK33*^{K102R} was generated by site-directed mutagenesis PCR (Ho et al., 1989) using primer pair CPK33-K102R-F/-R. To generate the *THI1* overexpression transgenic plants, the full-length cDNA of *THI1*, amplified by primer pair *THI1*OE-F/-R, was cloned into the binary vector pSTART. For the *THI1* RNAi construct, a 361-bp fragment was amplified using primers *THI1*Ri-F and *THI1*Ri-R, and inserted conversely into the vector pTCK303 (under the control of the *ZmUbiquitin* promoter). The plant transformation plasmids were introduced into *A. tumefaciens* GV3101 and used to transform Arabidopsis. The primers used are listed in Supplemental Table S1.

Drought Stress and Water Loss Experiments

For drought stress experiment, seeds were incubated in mixed soil (nutrient soil:vermiculite, 2:1, v/v) in a growth chamber with sufficient watering. Three weeks later, the plants were subjected to drought stress treatment by withholding water for 2 to 3 weeks. Then, plants were rehydrated for 3 d before the photograph was taken. For water loss measurement, rosette leaves were detached from 4-week-old plants, placed on a piece of weighing paper, and kept at 20°C and 50% humidity in the light. The leaves were weighed immediately after they were cut and periodically thereafter. The water loss rate was calculated on the basis of the initial fresh weight of the plants, with three replicates for each assay.

Yeast Two-Hybrid Screening

Yeast two-hybrid assays were based on the ProQuest Two-Hybrid System (Invitrogen). To screen for interacting proteins, full-length *THI1* cDNA was amplified using primers *THII*-Y2HF and *THII*-Y2HR, and cloned into pDEST32 vector as bait and transformed into yeast (*Saccharomyces cerevisiae*) strain Mav203 using the lithium acetate method. The cDNA library from the epidermal strips of 4-week-old Arabidopsis leaves fused to pDEST22 (complexity of 8.4×10^7 total recombinants) was transformed into yeast strain Mav203 carrying the THI1 bait. The transformed cells were plated on synthetic dropout selection medium that lacked Trp, Leu, and His supplemented with 30 mM 3-amino-1,2,4-triazole (Sigma-Aldrich) to reduce the appearance of false-positive colonies. After transformants (3.2×10^5) were screened for activation of the *HIS3*, *Uracil*, and *lacZ* reporter genes, plasmid DNA was recovered from the yeast cells using a TIANprep yeast plasmid DNA kit (Tiangen) and then transformed into *Escherichia coli* for sequencing.

To confirm the interaction, the full-length or kinase domain fragment of *CPK33* was cloned into pDEST22 as prey, and cotransformed with THI1 bait plasmid into yeast strain Mav203 according to the previously described procedure. Transformants showing the Ura$^+$, His$^+$, and LacZ$^+$ phenotypes will be identified as interacting protein pairs. The specific primers used to amplify the genes are listed in Supplemental Table S1.

Protein Expression and Purification

To create the His-tagged THI1 for bacterial expression, the full-length coding region of *THI1* was PCR amplified with the primer pairs *THI1*PF and *THI1*PR (Supplemental Table S1) and cloned into pET-30a vector. To express and purify GST-tagged CPK33 and CPK33^{K102R} proteins for kinase assay, the coding sequences were amplified from the above-described *CPK33* and *CPK33*^{K102R} constructs with primers *CPK33*PF and *CPK33*PR and cloned into pGXP-6P-1. The recombinant plasmids were transformed into the *E. coli* BL21 (DE3) strain. THI1-His fusion protein and CPK33-GST/ CPK33^{K102R} -GST fusion proteins were expressed and purified using Ni-NTA Purification System (Invitrogen) and Glutathione Sepharose 4B (GE), respectively. Purified proteins were quantified by Bio-Rad protein assay reagent.

In-Gel Kinase Assay

Kinase assays were carried out at 28°C for 15 min by incubating 1 μg of the purified CPK33-GST or CPK33^{K102R}-GST in 50 μL of buffer (25 mM Tris-HCl, pH 7.5, 10 mM $MgCl_2$, 10 μM ATP) containing 2 μCi of [γ-^{32}P]ATP. For substrate phosphorylation, 1 μg of CPK33-GST or CPK33^{K102R}-GST was incubated with 1 μg of the purified THI1-His or MBP protein (as general substrate; Sigma) for 15 min under the same condition. To analyze the inhibition of CPK33 kinase activity by THI1, 1 μg of CPK33-GST was incubated with 0.1, 1, 10, and 50 μg of THI1-His protein, and the same amount of GST protein was used as the negative control. The ^{32}P-labeled protein bands were visualized by the Variable Mode Imager Typhoon 8600 (Amersham Pharmacia Biotech).

GST Pull-Down Assay

For protein pull-down experiments, GST alone or GST-CPK33 (700 μg) was incubated with THI1-His (700 μg) in binding buffer (20 mM Tris-HCl, pH 7.5, 150 mM NaCl, 3 mM $MgCl_2$, 1 mM dithiothreitol, and 0.1% Triton X-100) at 4°C for 1 h. Then, 30 μL of immobilized glutathione beads were added and incubated for another 1 h at 4°C. After the beads were washed three times with PBS buffer, 4× loading buffer was added to the beads. The samples were boiled for 5 min, separated by 12% SDS-PAGE, and analyzed by immunoblotting with an anti-His antibody.

Coimmunoprecipitation Assay in *Nicotiana benthamiana*

Coimmunoprecipitation assay was performed as described (Choi et al., 2012) with minor modifications. In brief, the ORF sequences of *CPK33* and *THI1* were amplified by PCR using primer pair *CPK33*OE-F/-R and *THI1*-Y2HF/R and cloned into pCM1307-N-Myc and pB7WGF2.0, respectively. The resulting construct Myc-CPK33 or THI1-GFP was transformed into *Agrobacterium* strain GV3101 and suspended in infiltration buffer to OD_{600} = 0.8. Equal volumes of *Agrobacteria* carrying different constructs were mixed and coinfiltrated into the 3-week-old leaves of tobacco plants. The infiltrated tobacco plants were grown for an additional 3 d in a growth chamber under a 16-h-light/8-h-dark photoperiod at 28°C. Proteins were extracted from 1 g of leaf samples with 2 mL of extraction buffer (50 mM Tris-HCl, pH 8.0, 150 mM NaCl, 2 mM EDTA, 1 mM dithiothreitol, 10% glycerol, 1% Triton X-100, 1 mM PMSF, and 1× protease inhibitor cocktail [Roche]). The samples were left on ice with gentle shaking for 1 h to solubilize membrane proteins and centrifuged at 16,000*g* at 4°C for 30 min. Supernatants (1 mL) were incubated with 10 μL of anti-GFP polyclonal antibody (Sigma-Aldrich) for 2 h at 4°C with gentle rotation, and then 50 μL of 50% (v/v) protein A agarose bead (GE) slurry was added and incubated overnight. Following incubation, the beads were washed four times with washing buffer (1× PBS, 0.5% Triton X-100, 1× protease inhibitor cocktail). After the last centrifugation, the PBS buffer was removed completely. The pellet was resuspended in 2× SDS-PAGE loading buffer. Eluted proteins were analyzed by immunoblotting using anti-Myc antibody (Sigma-Aldrich) or anti-GFP monoclonal antibody (Sigma-Aldrich). Blots were developed using the SuperSignal West Pico Chemiluminescent kit (Pierce).

Accession Numbers

Sequence data from this article can be found in the Arabidopsis Genome Initiative database under the following accession numbers: At3g18780 (*ACTIN2*), At5g54770 (*THI1*), and At1g50700 (*CPK33*).

Supplemental Data

The following supplemental materials are available.

Supplemental Figure S1. Subcellular localization of THI1 in Arabidopsis mesophyll protoplasts treated with different concentrations of ABA.

Supplemental Figure S2. Subcellular localization of THI1 in Arabidopsis mesophyll protoplasts.

Supplemental Figure S3. Phenotype of *thi1* mutants.

Supplemental Figure S4. Phenotype of *THI1* knock-down (RNAi) plants.

Supplemental Figure S5. Stomatal movement of wild type under thiamine treatment.

Supplemental Figure S6. The determination of the optimal 3-amino-1,2,4-triazole concentration required for the yeast two-hybrid screen.

Supplemental Figure S7. THI1 interacts with CPK33 in a yeast two-hybrid assay under thiamine conditions.

Supplemental Figure S8. In vivo coimmunoprecipitation analysis of THI1 and CPK33 interaction in *N. benthamiana* leaves.

Supplemental Figure S9. Subcellular localization of CPK33 and CPK33^{G2A} in Arabidopsis mesophyll protoplasts.

Supplemental Figure S10. Subcellular localization analysis of THI1 in protoplasts of Col-0 and *cpk33* mutant.

Supplemental Figure S11. PCR-based validation of the *cpk33* mutants.

Supplemental Figure S12. In vitro kinase activity of CPK33^{K102R}.

Supplemental Figure S13. Peptide sequence alignment of CPK33 and its kinase homologs in Arabidopsis.

Supplemental Figure S14. Gene sequencing of CPK33 in wild-type and transgenic plants.

Supplemental Table S1. Primers used for PCR, RT-PCR, and qPCR analysis.

ACKNOWLEDGMENTS

We thank ABRC for providing seed of the T-DNA insertion mutants CS3573, CS3590, and Salk_036145. We also thank Sarah Assmann (Pennsylvania State University) for her valuable suggestions during the drafting of the article and Inhwan Hwang (Pohang University of Science and Technology, South Korea) for his helpful discussion and the p35S::H$^+$-ATPase-RFP vector used in this study.

Received October 23, 2015; accepted December 9, 2015; published December 10, 2015.

LITERATURE CITED

Acharya BR, Jeon BW, Zhang W, Assmann SM (2013) Open Stomata 1 (OST1) is limiting in abscisic acid responses of *Arabidopsis* guard cells. New Phytol **200:** 1049–1063

Ajjawi I, Tsegaye Y, Shintani D (2007) Determination of the genetic, molecular, and biochemical basis of the *Arabidopsis thaliana* thiamin auxotroph *th1*. Arch Biochem Biophys **459:** 107–114

Alonso JM, Stepanova AN, Leisse TJ, Kim CJ, Chen H, Shinn P, Stevenson DK, Zimmerman J, Barajas P, Cheuk R, et al (2003) Genome-wide insertional mutagenesis of *Arabidopsis thaliana.* Science **301:** 653–657

Belanger FC, Leustek T, Chu B, Kriz AL (1995) Evidence for the thiamine biosynthetic pathway in higher-plant plastids and its developmental regulation. Plant Mol Biol **29:** 809–821

Biller L, Matthiesen J, Kühne V, Lotter H, Handal G, Nozaki T, Saito-Nakano Y, Schümann M, Roeder T, Tannich E, et al (2014) The cell surface proteome of Entamoeba histolytica. Mol Cell Proteomics **13:** 132–144

Camoni L, Harper JF, Palmgren MG (1998) 14-3-3 proteins activate a plant calcium-dependent protein kinase (CDPK). FEBS Lett **430:** 381–384

Chabregas SM, Luche DD, Farias LP, Ribeiro AF, van Sluys MA, Menck CF, Silva-Filho MC (2001) Dual targeting properties of the N-terminal signal sequence of *Arabidopsis thaliana* THI1 protein to mitochondria and chloroplasts. Plant Mol Biol **46:** 639–650

Chabregas SM, Luche DD, Van Sluys MA, Menck CF, Silva-Filho MC (2003) Differential usage of two in-frame translational start codons regulates subcellular localization of *Arabidopsis thaliana* THI1. J Cell Sci **116:** 285–291

Chatterjee A, Jurgenson CT, Schroeder FC, Ealick SE, Begley TP (2007) Biosynthesis of thiamin thiazole in eukaryotes: conversion of NAD to an advanced intermediate. J Am Chem Soc **129:** 2914–2922

Cheng SH, Willmann MR, Chen HC, Sheen J (2002) Calcium signaling through protein kinases. The Arabidopsis calcium-dependent protein kinase gene family. Plant Physiol **129:** 469–485

Choi DS, Hwang IS, Hwang BK (2012) Requirement of the cytosolic interaction between PATHOGENESIS-RELATED PROTEIN10 and LEUCINE-RICH REPEAT PROTEIN1 for cell death and defense signaling in pepper. Plant Cell **24:** 1675–1690

Clough SJ, Bent AF (1998) Floral dip: a simplified method for Agrobacterium-mediated transformation of *Arabidopsis thaliana.* Plant J **16:** 735–743

DeFalco TA, Bender KW, Snedden WA (2010) Breaking the code: Ca^{2+} sensors in plant signalling. Biochem J **425:** 27–40

Farmer PK, Choi JH (1999) Calcium and phospholipid activation of a recombinant calcium-dependent protein kinase (DcCPK1) from carrot (*Daucus carota L.*). Biochim Biophys Acta **1434:** 6–17

Franz S, Ehlert B, Liese A, Kurth J, Cazalé AC, Romeis T (2011) Calcium-dependent protein kinase CPK21 functions in abiotic stress response in *Arabidopsis thaliana*. Mol Plant **4:** 83–96

French AP, Mills S, Swarup R, Bennett MJ, Pridmore TP (2008) Colocalization of fluorescent markers in confocal microscope images of plant cells. Nat Protoc **3:** 619–628

Geiger D, Maierhofer T, Al-Rasheid KA, Scherzer S, Mumm P, Liese A, Ache P, Wellmann C, Marten I, Grill E, et al (2011) Stomatal closure by fast abscisic acid signaling is mediated by the guard cell anion channel SLAH3 and the receptor RCAR1. Sci Signal **4:** ra32

Geiger D, Scherzer S, Mumm P, Marten I, Ache P, Matschi S, Liese A, Wellmann C, Al-Rasheid KA, Grill E, et al (2010) Guard cell anion channel SLAC1 is regulated by CDPK protein kinases with distinct Ca^{2+} affinities. Proc Natl Acad Sci USA **107:** 8023–8028

Geiger D, Scherzer S, Mumm P, Stange A, Marten I, Bauer H, Ache P, Matschi S, Liese A, Al-Rasheid KA, et al (2009) Activity of guard cell anion channel SLAC1 is controlled by drought-stress signaling kinase-phosphatase pair. Proc Natl Acad Sci USA **106:** 21425–21430

Gerdes S, Lerma-Ortiz C, Frelin O, Seaver SM, Henry CS, de Crécy-Lagard V, Hanson AD (2012) Plant B vitamin pathways and their compartmentation: a guide for the perplexed. J Exp Bot **63:** 5379–5395

Goyer A (2010) Thiamine in plants: aspects of its metabolism and functions. Phytochemistry **71:** 1615–1624

Grabov A, Leung J, Giraudat J, Blatt MR (1997) Alteration of anion channel kinetics in wild-type and *abi1-1* transgenic *Nicotiana benthamiana* guard cells by abscisic acid. Plant J **12:** 203–213

Hedrich R, Busch H, Raschke K (1990) Ca^{2+} and nucleotide dependent regulation of voltage dependent anion channels in the plasma membrane of guard cells. EMBO J **9:** 3889–3892

Ho SN, Hunt HD, Horton RM, Pullen JK, Pease LR (1989) Site-directed mutagenesis by overlap extension using the polymerase chain reaction. Gene **77:** 51–59

Jin JB, Bae H, Kim SJ, Jin YH, Goh CH, Kim DH, Lee YJ, Tse YC, Jiang L, Hwang I (2003) The Arabidopsis dynamin-like proteins ADL1C and ADL1E play a critical role in mitochondrial morphogenesis. Plant Cell **15:** 2357–2369

Johnson DR, Bhatnagar RS, Knoll LJ, Gordon JI (1994) Genetic and biochemical studies of protein N-myristoylation. Annu Rev Biochem **63:** 869–914

Kawamoto N, Sasabe M, Endo M, Machida Y, Araki T (2015) Calcium-dependent protein kinases responsible for the phosphorylation of a bZIP transcription factor FD crucial for the florigen complex formation. Sci Rep **5:** 8341–8349

Kim DH, Eu YJ, Yoo CM, Kim YW, Pih KT, Jin JB, Kim SJ, Stenmark H, Hwang I (2001) Trafficking of phosphatidylinositol 3-phosphate from the trans-Golgi network to the lumen of the central vacuole in plant cells. Plant Cell **13:** 287–301

Kim TH, Böhmer M, Hu H, Nishimura N, Schroeder JI (2010) Guard cell signal transduction network: advances in understanding abscisic acid, CO_2, and Ca^{2+} signaling. Annu Rev Plant Biol **61:** 561–591

Lee SC, Lan W, Buchanan BB, Luan S (2009) A protein kinase-phosphatase pair interacts with an ion channel to regulate ABA signaling in plant guard cells. Proc Natl Acad Sci USA **106:** 21419–21424

Lee SC, Lim CW, Lan W, He K, Luan S (2013) ABA signaling in guard cells entails a dynamic protein-protein interaction relay from the PYL-RCAR family receptors to ion channels. Mol Plant **6:** 528–538

Lee SC, Luan S (2012) ABA signal transduction at the crossroad of biotic and abiotic stress responses. Plant Cell Environ **35:** 53–60

Li CL, Wang M, Ma XY, Zhang W (2014) NRGA1, a putative mitochondrial pyruvate carrier, mediates ABA regulation of guard cell ion channels and drought stress responses in *Arabidopsis*. Mol Plant **7:** 1508–1521

Li J, Wang XQ, Watson MB, Assmann SM (2000) Regulation of abscisic acid-induced stomatal closure and anion channels by guard cell AAPK kinase. Science **287:** 300–303

Liu S, Liu S, Wang M, Wei T, Meng C, Wang M, Xia G (2014) A wheat *SIMILAR TO RCD-ONE* gene enhances seedling growth and abiotic stress resistance by modulating redox homeostasis and maintaining genomic integrity. Plant Cell **26:** 164–180

Lu CS, Hodge JJ, Mehren J, Sun XX, Griffith LC (2003) Regulation of the Ca^{2+}/CaM-responsive pool of CaMKII by scaffold-dependent autophosphorylation. Neuron **40:** 1185–1197

Ma SY, Wu WH (2007) AtCPK23 functions in Arabidopsis responses to drought and salt stresses. Plant Mol Biol **65:** 511–518

Machado CR, de Oliveira RL, Boiteux S, Praekelt UM, Meacock PA, Menck CF (1996) *Thi1*, a thiamine biosynthetic gene in *Arabidopsis thaliana*, complements bacterial defects in DNA repair. Plant Mol Biol **31:** 585–593

Machado CR, Praekelt UM, de Oliveira RC, Barbosa AC, Byrne KL, Meacock PA, Menck CF (1997) Dual role for the yeast *THI4* gene in thiamine biosynthesis and DNA damage tolerance. J Mol Biol **273:** 114–121

Macrobbie EA (1997) Signalling in guard cells and regulation of ion channel activity. J Exp Bot **48:** 515–528

Mori IC, Murata Y, Yang Y, Munemasa S, Wang YF, Andreoli S, Tiriac H, Alonso JM, Harper JF, Ecker JR, et al (2006) CDPKs CPK6 and CPK3 function in ABA regulation of guard cell S-type anion- and $Ca^{(2+)}$-permeable channels and stomatal closure. PLoS Biol **4:** e327

Pandey S, Zhang W, Assmann SM (2007) Roles of ion channels and transporters in guard cell signal transduction. FEBS Lett **581:** 2325–2336

Papini-Terzi FS, Galhardo RS, Farias LP, Menck CF, Van Sluys MA (2003) Point mutation is responsible for Arabidopsis *tz-201* mutant phenotype affecting thiamin biosynthesis. Plant Cell Physiol **44:** 856–860

Pei ZM, Kuchitsu K, Ward JM, Schwarz M, Schroeder JI (1997) Differential abscisic acid regulation of guard cell slow anion channels in Arabidopsis wild-type and *abi1* and *abi2* mutants. Plant Cell **9:** 409–423

Pei ZM, Ward JM, Harper JF, Schroeder JI (1996) A novel chloride channel in *Vicia faba* guard cell vacuoles activated by the serine/threonine kinase, CDPK. EMBO J **15:** 6564–6574

Rapala-Kozik M, Wolak N, Kujda M, Banas AK (2012) The upregulation of thiamine (vitamin B1) biosynthesis in *Arabidopsis thaliana* seedlings under salt and osmotic stress conditions is mediated by abscisic acid at the early stages of this stress response. BMC Plant Biol **12:** 2–15

Raschke M, Bürkle L, Müller N, Nunes-Nesi A, Fernie AR, Arigoni D, Amrhein N, Fitzpatrick TB (2007) Vitamin B1 biosynthesis in plants requires the essential iron sulfur cluster protein, THIC. Proc Natl Acad Sci USA **104:** 19637–19642

Ribeiro DT, Farias LP, de Almeida JD, Kashiwabara PM, Ribeiro AF, Silva-Filho MC, Menck CF, Van Sluys MA (2005) Functional characterization of the *thi1* promoter region from *Arabidopsis thaliana*. J Exp Bot **56:** 1797–1804

Ronzier E, Corratgé-Faillie C, Sanchez F, Prado K, Brière C, Leonhardt N, Thibaud JB, Xiong TC (2014) CPK13, a noncanonical Ca^{2+}-dependent protein kinase, specifically inhibits KAT2 and KAT1 shaker K^+ channels and reduces stomatal opening. Plant Physiol **166:** 314–326

Savvides A, Fanourakis D, van Ieperen W (2012) Co-ordination of hydraulic and stomatal conductances across light qualities in cucumber leaves. J Exp Bot **63:** 1135–1143

Schaller GE, Harmon AC, Sussman MR (1992) Characterization of a calcium- and lipid-dependent protein kinase associated with the plasma membrane of oat. Biochemistry **31:** 1721–1727

Scherzer S, Maierhofer T, Al-Rasheid KA, Geiger D, Hedrich R (2012) Multiple calcium-dependent kinases modulate ABA-activated guard cell anion channels. Mol Plant **5:** 1409–1412

Schroeder JI, Hedrich R (1989) Involvement of ion channels and active transport in osmoregulation and signaling of higher plant cells. Trends Biochem Sci **14:** 187–192

Schroeder JI, Keller BU (1992) Two types of anion channel currents in guard cells with distinct voltage regulation. Proc Natl Acad Sci USA **89:** 5025–5029

Sheen J (2001) Signal transduction in maize and Arabidopsis mesophyll protoplasts. Plant Physiol **127:** 1466–1475

Tunc-Ozdemir M, Miller G, Song L, Kim J, Sodek A, Koussevitzky S, Misra AN, Mittler R, Shintani D (2009) Thiamin confers enhanced tolerance to oxidative stress in *Arabidopsis*. Plant Physiol **151:** 421–432

Verslues PE, Bray EA (2006) Role of abscisic acid (ABA) and Arabidopsis thaliana ABA-insensitive loci in low water potential-induced ABA and proline accumulation. J Exp Bot **57:** 201–212

Wang XQ, Ullah H, Jones AM, Assmann SM (2001) G protein regulation of ion channels and abscisic acid signaling in *Arabidopsis* guard cells. Science **292:** 2070–2072

Zhang W, Nilson SE, Assmann SM (2008) Isolation and whole-cell patch clamping of Arabidopsis guard cell protoplasts. CSH Protoc **2008:** pdb prot5014

Zhu SY, Yu XC, Wang XJ, Zhao R, Li Y, Fan RC, Shang Y, Du SY, Wang XF, Wu FQ, et al (2007) Two calcium-dependent protein kinases, CPK4 and CPK11, regulate abscisic acid signal transduction in *Arabidopsis*. Plant Cell **19:** 3019–3036

Zou JJ, Wei FJ, Wang C, Wu JJ, Ratnasekera D, Liu WX, Wu WH (2010) Arabidopsis calcium-dependent protein kinase CPK10 functions in abscisic acid- and Ca^{2+}-mediated stomatal regulation in response to drought stress. Plant Physiol **154:** 1232–1243